Journal of Ceramic Processing Research. Vol. 8, No. 1, pp. 59~63 (2007)

J O U R N A L O F
Ceramic Processing Research

Effect of deposition temperature on electro-optical properties of SnO_2 thin films fabricated by a PECVD method

Jeong-Hoon Lee[a], Gun-Eik Jang[a,*], Dae-Ho Yoon[b] and Sang-Hee Son[c]

[a]*Department of Advanced Materials Engineering, Chungbuk National University, Cheongju 361-763, Korea*
[b]*School of Metallurgical & Materials Engineering, Sungkyunkwan University, Suwon 440-746, Korea*
[c]*Division of Information and Engineering Telecommunication, Cheong-ju University, Cheongju 360-764, Korea*

Tin oxide (SnO_2) thin films were prepared on glass substrates by a Plasma Enhanced Chemical Vapor Deposition (PECVD) method at different temperatures. The XRD data indicate that films are polycrystalline SnO_2, which is in the tetragonal system with a rutile-type structure. As the deposition temperature was increased, the texture plane of a film changed from the (200) plane to denser (211) and (110) planes. SnO_2 thin films prepared at 275 ºC have a high resistivity of 1.07×10^{-1} Ω·cm and low transmittance of 69.78%. On the other hand, SnO_2 thin films deposited at 325~425 ºC show an electrical resistivity of ~10^{-2} Ω·cm and a transmission coefficient between 80% and 85% in most of the visible spectrum. The properties of SnO_2 films were critically affected by the deposition temperature.

Key words: tin oxide, PECVD, transmittance, resistivity.

Introduction

Tin(IV) oxide is an oxygen-defect type of semiconductor with a wide band gap (3.7 eV) and a high mobility. The compound is transparent in the visible region and reflective in the infrared region [1-2]. The unique physical property of SnO_2 thin films with a tetragonal structure with it superior chemical stability, has allowed its promising in applications for various devices, such as gas sensors, liquid crystal displays, transparent conducting electrodes, and solar cells [3-4]. Various processing routes, both physical and chemical deposition methods, have been utilized to prepare SnO_2 thin films, including pulsed laser deposition, radio frequency sputtering, a sol-gel process, spray pyrolysis, electron beam evaporation and PECVD [5-7]. Among them, PECVD was chosen as an ideal fabrication method in order to obtain nano-structured SnO_2 thin films basically due to its low deposition temperature.

It was known that especially for gas sensor applications, SnO_2 thin films need to have a small grain size and a high surface-to-volume ratio in order to enhance their reliability and electrical properties [8]. It was also proven that microstructural optimization of sensor materials to achieve small grain size and large surface area was an effective way to obtain high sensitivity and selectivity for SnO_2-based gas sensors. Therefore, it is necessary to know how the process parameters affect the microstructure of SnO_2 thin films.

In the present study, SnO_2 thin films have been fabricated by a PECVD method and the effects of deposition temperature on the microstructure, electrical and optical properties of the SnO_2 thin films were systematically studied.

Experimental

Figure 1 shows a schematic of the apparatus of the remote PECVD system. The apparatus is composed of a reaction chamber, reaction gas supply system, vacuum

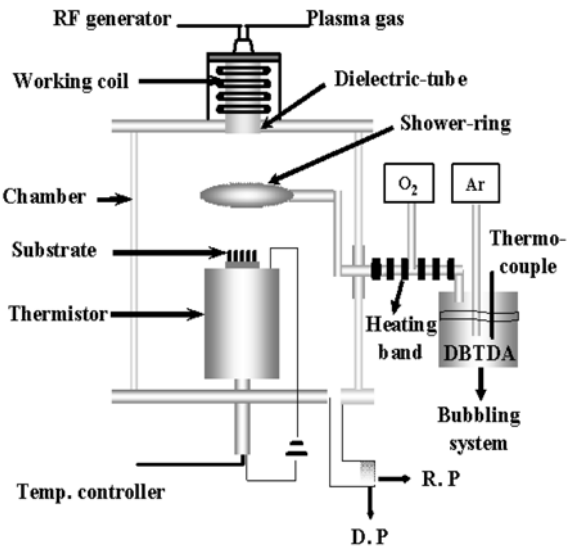

Fig. 1. A schematic of the apparatus of the remote plasma enhanced chemical vapor deposition system.

*Corresponding author:
Tel : +82-43-261-2412
Fax: +82-43-274-8925
E-mail: gejang@chungbuk.ac.kr

pump and radio frequency (RF) power supply system. The reaction gas supply system is composed of the mass flow controller (MFC), tin source (dibutyl tin diacetate) bubbling subsystem and needle valve. An Inductively coupled plasma (ICP) was used as the plasma source and it was generated by a 13.56 MHz, ~1.5 kW RF generator.

The substrate was initially cleaned by acetone in a supersonic wave cleaner and then placed into a vacuum chamber. Following that, Ar ion etching under a power input of 50 W was performed on the substrate for 20 minutes prior to deposition. The Ar ion etching not only cleaned the surface of the substrate but also improved the adhesion between the films and the substrates. The metal-organic compound dibutyl tin diacetate (Aldrich, 98% purity), $(C_4H_9)_2$-Sn$(OOCCH_3)_2$, was used as the tin source material. Table 1 describe the detailed properties of dibutyl tin diacetate.

Since dibutyl tin diacetate exists in the liquid state at room temperature, dibutyl tin diacetate was soaked at 98 °C. dibutyl tin diacetate steam can be carried into the reaction chamber by bubbling Ar gas (99.99%) through it. Ar was used as the carrier gas at a flow rate of 100 sccm and 40 sccm O_2 was used as the reaction gas. Finally, the SnO_2 thin films were deposited on the substrate at different temperatures from 275 °C to 425 °C under a plasma discharge aroused by RF power.

The crystalline phases of the thin films were identified by an X-ray diffractometer (Scintag XDS 2000). The microstructure and surface roughness were observed by field emission scanning electron microscope (Hitachi S 2500C) and an atomic force microscope (Digital Instruments Nanoscope III), respectively. The electrical properties of the films were studied at room temperature by Hall effect measurements (Lakeshore, 7507) under the magnetic field of 5 kG. The transmittance of thin films was measured using an UV-visible spectrometer (Shimadzu, UV-3100) in the range of wave length 300~800 nm. The dynamic conductance temperature measurement of the samples was carried out under an air flow for the temperature range of 25~300 °C.

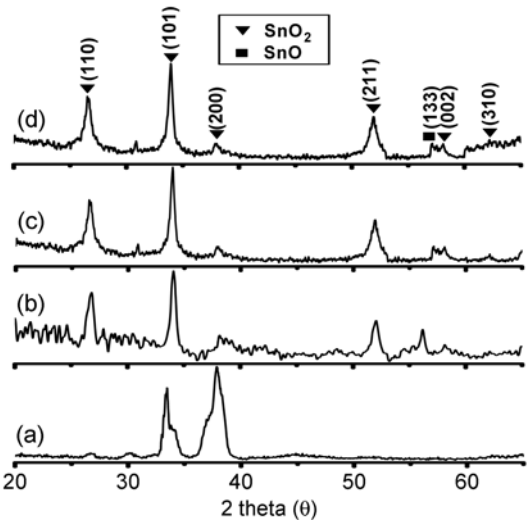

Fig. 2. XRD patterns as a function of deposition temperatures: (a) 275 °C (b) 325 °C (c) 375 °C and (d) 425 °C

Results

Figure 2 Shows the XRD diffraction patterns of SnO_2 films grown at substrate temperatures of 275, 325, 375 and 425 °C. Based on these XRD analyses, the films are polycrystalline in nature and consisted of a single phase of SnO_2 (cassiterite) with the rutile structure. The films grown at 275 °C have little crystallinity with a broad (200) peak as the major peak; whereas those grown at 325 °C exhibit a better crystallinity, and still better as the temperature increased from 325 to 425 °C. The best crystallinity was obtained at 425 °C, a deposition temperature in which a highly oriented (101) growth occurs. Interestingly, as the substrate increased from 275 to 325 °C, the preferred orientation changed from (200) and (101) to (110) and (101).

Figure 3 shows the cross-sectional and surface FE-SEM micrographs of SnO_2 thin films. The SnO_2 thin films prepared at 275 °C are composed of a non-uniform island structure with different sizes [Fig. 3(a)]. As the deposition temperature increased above 325 °C, the film microstructure changed into a compact structure with a high film density. The SnO_2 thin films deposited at 325~425 °C showed a granular structure with nano-grains of a size of 18~25 nm. From the cross sectional view, the grains in the films appear to have a columnar structure [Fig. 3(b)~(d)]. The SnO_2 thin film deposited at 325 °C was very dense and the grain size was about 14 nm. With the deposition temperature increased to 425 °C, the surface of the as-deposited films became rough and the grain size increased to about 25 nm. This phenomenon is considered to have occurred because of the nucleation and growth due to the thermal activation with the increase of deposition temperature.

In Fig. 4, the AFM micrographs show the morphology of SnO_2 films deposited on glass substrates at 4 different temperatures. The surface morphology observed in Fig. 4 suggests a micro structural change of tin oxide grown on glass substrates with oxidation temperature. That is,

Table 1. The properties of DBTDA

Formula	T_m (°C)	T_b (°C)	D (g/mL)	vapor pressure (mmHg)	vapor density	phase
$(C_4H_9)_2$-Sn$(OOCCH_3)_2$	7~10	142~145 (at 10 mmHg)	1.32 (at 25 °C)	1.3 (at 25 °C)	12 (vs air)	Liquid

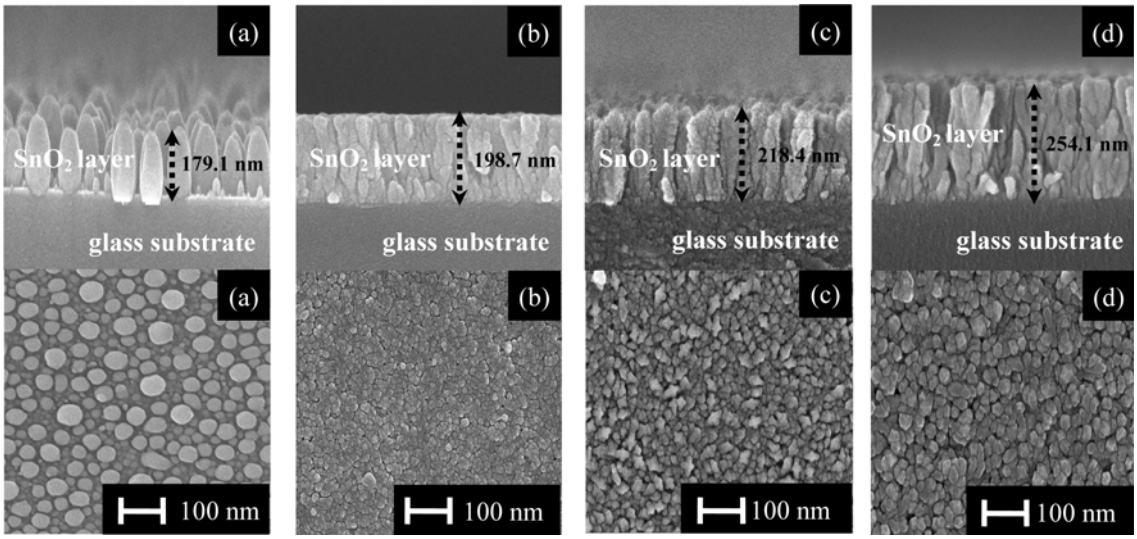

Fig. 3. Morphologies of surface and cross-sectional area of thin films as a function of deposition temperature: (a) 275 °C (b) 325 °C (c) 375 °C and (d) 425 °C

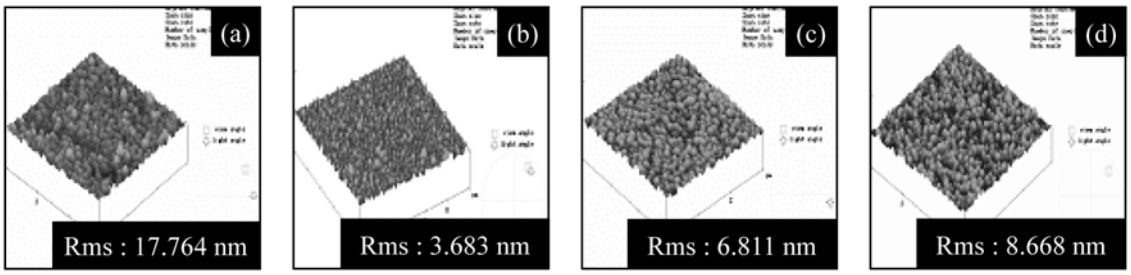

Fig. 4. Surface roughness of thin films as a function of deposition temperature: (a) 275 °C (b) 325 °C (c) 375 °C and (d) 425 °C

Table 2. Resistivity, carrier concentration and mobility of the SnO_2 thin films as a function of deposition temperature

Deposition temperature (°C)	Hall coefficient			Type
	Resistivity (Ω·cm)	Concentration (cm^{-3})	Mobility ($cm^2/V·s$)	
275	1.07×10^{-1}	-4.4×10^{-17}	4.81	N
325	2.95×10^{-2}	-4.2×10^{-19}	11.43	N
375	3.57×10^{-2}	-1.9×10^{-19}	13.81	N
425	5.54×10^{-2}	-5.8×10^{-18}	16.85	N

the surface roughness of the films increases linearly with deposition temperature. The RMS value indicating the amount of roughness was 3.683 for the film deposited at 325 °C. However the RMS value shows a systematic trend of an increase with an increase of the deposition temperature. This can be explained by the preferred orientation during the grain-growth as the deposition temperature increased [9].

The effects of the deposition temperature on the carrier concentration, the mobility and the resistivity are shown in Fig. 5 and all the results are summarized in Table 2. Figure 5 suggests that the SnO_2 thin films grown at deposition temperatures of 275~425 °C are typical n-type conducting, with carrier concentration as high as from -4.4×10^{-17} to -4.2×10^{-19} cm^{-3}. However, the carrier

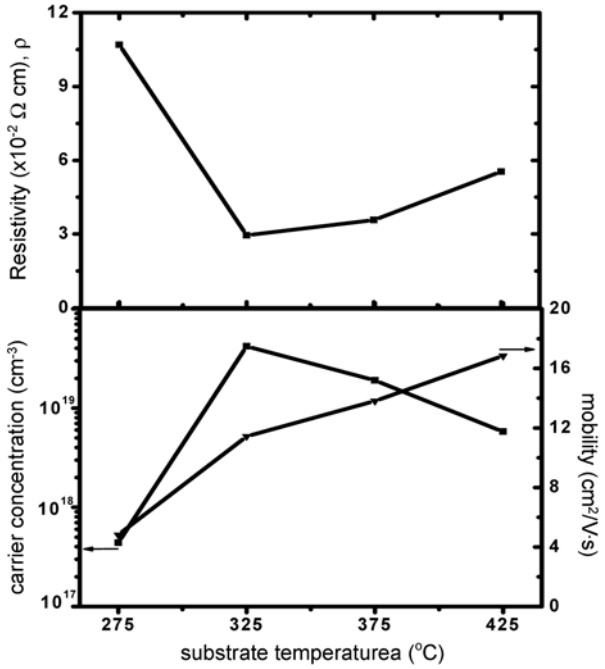

Fig. 5. Resistivity, carrier concentration and mobility of the SnO_2 thin films as a function of deposition temperature.

concentration decreases as the deposition temperature increases. This temperature dependence of electrical

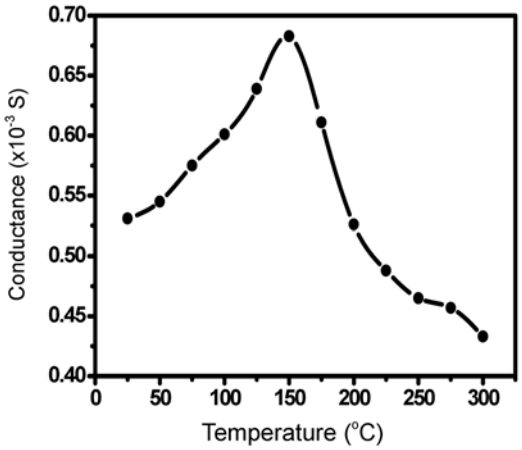

Fig. 6. Electrical conductance of the SnO_2 thin films as a function of temperature.

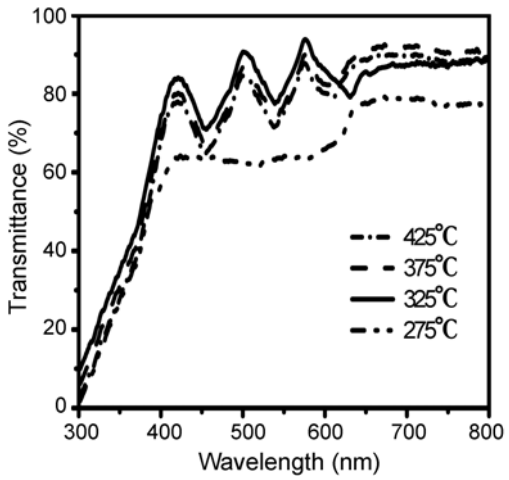

Fig. 7. Transmittance of the SnO_2 thin films as a function of deposition temperature.

property can be explained by considering the existence of donors (intrinsic defects such as oxygen vacancies and tin interstitials) in the films. At deposition temperatures higher than 325 °C, the carrier concentrations decreased because of the decreased intrinsic defects at higher deposition temperatures. Based on the results of electrical measurements, the resistivity and the mobility increased continuously with an increase of deposition temperature in the temperature ranges of 325~425 °C. This also can be explained by a decrease of carrier concentration with an increase of deposition temperature. Additionally the increases of mobility with the increases of deposition temperature can be explained as due to the grain boundary scattering effect reported by Shanthi et al. [10]. In other words, the increase of grain size as the deposition temperature increases reduces the grain boundary scattering of the electrons.

Figure 6 shows the electrical conductance temperature measurements of a sample with a heating rate of 1 K minute^{-1} under air. The conductance of the film shows a similar result. The conductance reaches its maximum at around 150 °C and then decreases while the temperature is increased continuously. Below 150 °C, the sample conductance exhibits the n-type semiconductor behavior of SnO_2. However above 150 °C, the oxygen starts to chemisorb on the sample surface in the form of O^- and O^{2-}, which derives electrons from the conduction band and thereby causes a decreasing trend in the film conductance. A similar result was reported by Liu et al. [11] for ultrafine tin oxide powders prepared by PECVD.

Figure 7 shows the transmission spectrum of the SnO_2 films of about 2000 Å thickness grown on glass at 275~425 °C. In case of the thin film deposited at 275 °C, this shows low transmittance of about 69.78% and a transmittance curve of fluid form with little amplitude. This can be explained in terms of low crystallinity and low surface density and diffuse scattering caused by the rough surface structure of film. Also it was found that SnO_2 films deposited at 325~425 °C have a transmission coefficient between 80% and 85% in most of the visible spectrum. It can be concluded that thin films that are dense with smooth surfaces have a high transmittance but the visible transmission is not much affected by the deposition temperature in the range of 325~425 °C. Another feature seen in Fig. 7 is a shift of the absorption edge to shorter wavelength depending on deposition temperature. The reason for the absorption edge shift to shorter wavelengths can be explained by the increase of carrier concentration of deposited thin films [12].

Conclusions

Tin oxide thin films were fabricated using a PECVD method at deposition temperatures of 275, 325, 375, and 425 °C. XRD results showed the films were the rutile structure and the crystallinity of the SnO_2 thin film increased with increasing deposition temperature. SnO_2 thin films prepared at 275 °C have a high resistivity of 1.07×10^{-1} Ω·cm and low transmittance of 69.78%. As the deposition temperature increased above 325 °C, the film microstructure was changed into a compact structure with high film density. SnO_2 thin films deposited at 325~425 °C have an electrical resistivity of ~10^{-2} Ω·cm and transmission coefficient between 80% and 85% in most of the visible spectrum. Additionally it was confirmed that SnO_2 thin film deposited at lower temperature 325~425 °C have a small grain size, low surface roughness and resistivity, and high transmittance. We can conclude that the optimized thin films using dibutyltin diacetate could be prepared at a deposition temperature of 325 °C.

Acknowledgment

This work was supported by the Regional Research Centers Program of the Ministry of Education & Human Resources Development.

References

1. E. Shanthi, V. Dutta, A. Banerjeer, and K.L. Chopra, J. Appl. Phys. 51[12] (1981) 6243-6251.
2. F.J. Yusta, M.L. Hitchman, and H. Shamlian, J. Mater. Chem. 7[8] (1997) 1421-1427.
3. D. Belanger, J.P. Dodelet, B.A. Lombos, and J.I. Dickson, J. Electrochem. Soc. 132[6] (1985) 1398-1405.
4. K.H. Kim, and C.G. Park, J. Electrochem. Soc. 138[8] (1991) 2408-2412.
5. J. Kane, H.P. Schweizer, and W. Kern, J. Electrochem. Soc. 123[2] (1976) 270-277.
6. G. Shanon, R. Rup, and A. Mansingh, Thin Solid Films 190[2] (1990) 287-301.
7. D.J. Goyal, S. Agashe, B.R. Marathe, M.G. Takwale, and V.G. Bhide, J. Appl. Phys. 73[11] (1993) 7520-7523.
8. J.I. Jung, B.C. Kim, S.H. Chang, and J.J. Kim, J. Kor. Ceram. Soc. 34[12] (1997) 1221-1226.
9. S. Shirakata, A. Yokoyama, and S. Isomura, Jpn, J. Appl. Phys. 35 (1996) 722-724.
10. S. Shanthi, C. Subramanian, and P. Ramasamy, J. Crystal Growth 197[4] (1999) 858-864.
11. Y. Liu, W. Zhu, O.K. Tan, and X. Yao, J. Mater. Sci.:Mater. Electron. 7[4] (1996) 279-282.
12. M. Ichimura, K. Shibayama, and K. Masui, Thin Solid Films 466[1-2] (2004) 34-36.